THE JOURNAL OF BIOLOGICAL CHEMISTRY VOL. 284, NO. 21, pp. 13987–13994, May 22, 2009

MDM2 Acts Downstream of p53 as an E3 Ligase to Promote FOXO Ubiquitination and Degradation*

Received for publication, March 17, 2009 Published, JBC Papers in Press, March 25, 2009, DOI 10.1074/jbc.M901758200

Wei Fu[‡], Qiuping Ma[‡], Lei Chen[‡], Pengfei Li[‡], Mu Zhang[‡], Sivapriya Ramamoorthy[§], Zafar Nawaz[§], Tsukasa Shimojima[¶], Hengbin Wang[¶], Yonghua Yang[‡1], Zheng Shen[‡], Yingtao Zhang[‡], Xiaohong Zhang[‡‖], Santo V. Nicosia[‡], Yanping Zhang[‡‡], Jack W. Pledger[§**], Jiandong Chen[§**], and Wenlong Bai[‡‖2]**

*From the Departments of [‡]Pathology and Cell Biology, University of South Florida College of Medicine, Tampa, Florida 33612, the Programs of [‖]Molecular Oncology and **Experimental Therapeutics, H. Lee Moffitt Cancer Center, Tampa, Florida 33612, the [§]Department of Biochemistry and Molecular Biology, University of Miami School of Medicine, Miami, Florida 33136, the [¶]Department of Biochemistry and Molecular Genetics, University of Alabama at Birmingham, Birmingham, Alabama 35233, and the [‡‡]Department of Radiation Oncology, University of North Carolina, Chapel Hill, North Carolina 27514*

Members of the FOXO (forkhead O) class of transcription factors are tumor suppressors that also control aging and organismal life span. Mammalian FOXO degradation is proteasome-mediated, although the ubiquitin E3 ligase for FOXO factors remains to be defined. We show that MDM2 binds to FOXO1 and FOXO3A and promotes their ubiquitination and degradation, a process apparently dependent on FOXO phosphorylation at AKT sites and the E3 ligase activity of MDM2. Binding of MDM2 to FOXO occurs through the region of MDM2 that directs its cellular trafficking and the forkhead box of FOXO1. MDM2 promotes the ubiquitination of FOXO1 in a cell-free system, and its knockdown by small interfering RNA causes accumulation of endogenous FOXO3A protein in cells and enhances the expression of FOXO target genes. In cells stably expressing a temperature-sensitive p53 mutant, activation of p53 by shifting to permissive temperatures leads to MDM2 induction and degradation of endogenous FOXO3A. These data suggest that MDM2 acts as an ubiquitin E3 ligase, downstream of p53, to regulate the degradation of mammalian FOXO factors.

FOXO (forkhead O) proteins belong to the family of forkhead transcriptional factors, which are characterized by a conserved DNA binding domain termed the "Forkhead box" (1). Mammalian FOXO factors include FOXO1 (previously known as FKHR), FOXO3A (previously known as FKHRL1), FOXO4 (previously known as AFX), and FOXO6. These factors control the expression of a variety of genes that regulate essential cellular processes, such as cell cycle (2–4), apoptosis (5), oxidative stress (6, 7), atrophy (8), energy homeostasis, and glucose metabolism (9, 10). Whole organism studies in worms and flies show that FOXO factors have conserved ability to increase the organismal longevity (11). Genetic and functional analysis identifies FOXO1 as a tumor suppressor in the prostate (12). Knock-out studies show that mammalian FOXO factors act redundantly to suppress tumorigenesis in a lineage-specific fashion (13) and to maintain the long term regenerative potential of hematopoietic stem cells by regulating genes involved in the cellular response to physiological oxidative stresses (14).

The transcription of FOXO factors is regulated by posttranslational modifications, including phosphorylation, acetylation, and ubiquitination. Multiple kinases, including AKT (15, 16), serum- and glucocorticoid-induced kinase (17), casein kinase 1 (18), mammalian Ste20-like kinase 1 (19), IκB kinase (20), and cyclin-dependent kinase 2 (21), catalyze FOXO phosphorylation and often promote FOXO nuclear exportation. In response to insulin and growth factors, FOXO1 and FOXO3A are ubiquitinated and degraded by the proteasome pathway after phosphorylation at known AKT sites (15, 22, 23). Acetyltransferases, p300 (24) and CBP (25), and SIRT1 deacetylase (26, 27) regulate the activity of FOXO through acetylation/deacetylation. The role of FOXO acetylation is controversial, but it could affect their nuclear retention (28), phosphorylation (25), and ubiquitination-mediated degradation (29). Moreover, these studies suggest that major posttranslational modifications of FOXO converge on ubiquitin-mediated degradation, which places the putative E3[3] ubiquitin ligases for FOXO factors at central stage regarding the overall cellular activity of FOXO factors.

MDM2 is an oncogene that is transcriptionally induced by the p53 tumor suppressor. In turn, MDM2 serves as an E3 ubiquitin ligase for p53, promoting its ubiquitination and degradation (30). Genetic analysis shows that the lethality of MDM2 null mice is rescued by simultaneous deletion of the p53, suggesting that the p53 is the major substrate for MDM2 in normal mouse development (31). However, MDM2 has been reported

* This work was supported, in whole or in part, by National Institutes of Health Grants CA93666 (to W. B.) and CA111334 (to W. B.). This work was also supported by Department of Defense Prostate Cancer Grant DAMD17-02-1-0140 (to W. B.) and American Heart Association Predoctoral Fellowship 0315115B (to W. F.).

[1] Present address: Medical College of Georgia Cancer Center, 1120 15th St., CN 2101A, Augusta, GA 30912.

[2] To whom correspondence should be addressed: Dept. of Pathology and Cell Biology, University of South Florida College of Medicine, 12901 Bruce B. Downs Blvd., MDC 11, Tampa, FL 33612-4799. Fax: 813-974-5536; E-mail: wbai@health.usf.edu.

[3] The abbreviations used are: E3, ubiquitin-protein isopeptide ligase; E1, ubiquitin-activating enzyme; MEF, mouse embryo fibroblast; GFP, green fluorescent protein; PBS, phosphate-buffered saline; DAPI, 4′,6′-diamidino-2-phenylindole; NTA, nitrilotriacetic acid; GST, glutathione *S*-transferase; HA, hemagglutinin; TRAIL, tumor necrosis-related apoptosis-inducing ligand; FACS, fluorescence-activated cell sorting; NLS, nuclear localization sequence; siRNA, small interfering RNA; shRNA, short hairpin RNA.

to exert p53-independent functions in various cellular processes and to contribute to the transformed phenotype in the absence of wild type p53 (32). Consistently, MDM2 controls the ubiquitination and degradation of numerous proteins with essential roles in tumorigenesis (33). In the present study, we report that MDM2 acts downstream of p53 as an E3 ligase for

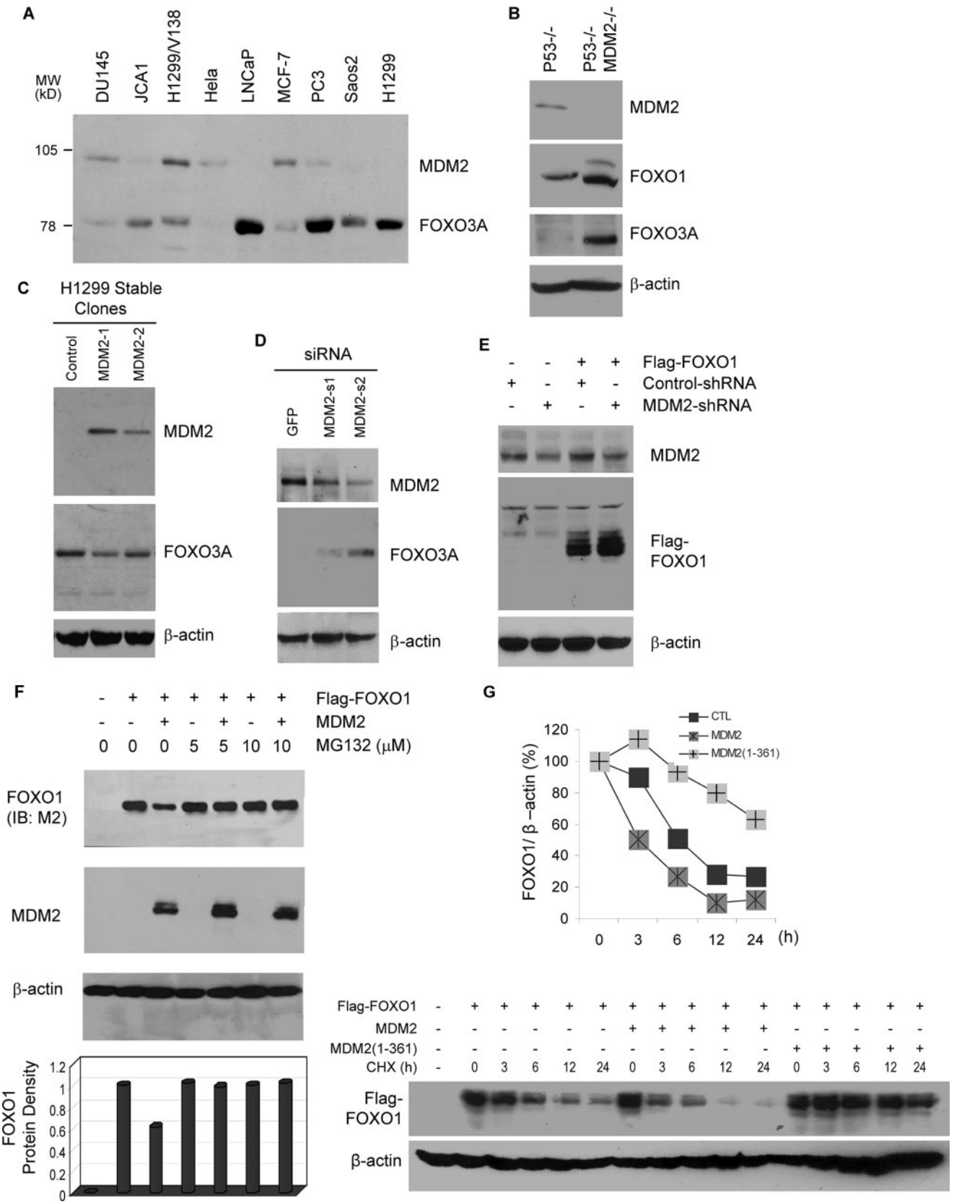

mammalian FOXO factors, which promotes the ubiquitination and degradation of FOXO1 and FOXO3A. The findings implicate a cross-talk between p53 and FOXO factors in regulating cellular responses to genotoxic stress and in tumorigenesis.

MATERIALS AND METHODS

Chemicals, Antibodies, and Cell Lines—Cycloheximide was purchased from Sigma, and MG132 was purchased from Calbiochem. Antibodies against FOXO1 (H-128 from Santa Cruz Biotechnology, Inc., Santa Cruz, CA), FOXO3A (H-144 from Santa Cruz Biotechnology), MDM2 (SMP14 from Santa Cruz Biotechnology; 2A10 from Calbiochem), c-Myc (A-14 from Santa Cruz Biotechnology), FLAG (M2-A-2220 and F-7452 from Sigma), HA (MMS-101P and PRB-101P from Covance), manganese superoxide dismutase (Upstate Biotechnology, Inc.), tumor necrosis-related apoptosis-inducing ligand (TRAIL; BD Pharmingen), p27 (N-20 from Santa Cruz), and β-actin (AC-74 from Sigma) were all obtained from commercial sources.

H1299/V138 cells were cultured as described (34). DU145, JCA1, PC3, HeLa, MCF-7, Saos-2, H1299, and p53 null mouse embryonic fibroblasts (MEFs) and p53 and MDM2 double null MEFs (35–37) were maintained in Dulbecco's modified Eagle's medium with 10% fetal bovine serum. LNCaP cells were cultured in RPMI 1640 with 10% fetal bovine serum. H1299 cells stably expressing human MDM2 were generated by cotransfecting MDM2 with pcDNA3 and selecting in the presence of 750 μg/ml G418.

Plasmids—pcDNA3-FLAG-FOXO1, pcDNA3-FLAG-FOXO1 (AAA), HA-FOXO3A, HA-FOXO3A (AAA), pcMDM2, and different MDM2 mutants were described previously (38–41). To construct pcDNA3-HA-FOXO1-(1–150), the FOXO1 cDNA fragment coding the first 150 amino acids was amplified by PCR with primers 5′-CGG GGG TCA CCG GAT CCA TGG CCG AGG C-3′ and 5′-GCG GCG GGA CGA TCT AGA CTA GCG CGG CTG C-3′, which generated BamHI and XbaI sites at 5′- and 3′-ends of the DNA fragment, respectively. The amplified FOXO1-(1–150) fragment was cloned into the BamHI and XbaI sites of pcDNA3.1 HA vector (Invitrogen). pcDNA3-HA-FOXO1-(1–270) and pcDNA3-HA-FOXO1-(256–655) were constructed similarly by generating a BamHI site at the 5′-end and a XbaI site at the 3′-end of the corresponding FOXO1 cDNA fragments. The upstream primer for FOXO1-(1–270) was the same as the FOXO1-(1–150), and the downstream primer was 5′-CTT GGC TCT AGA AGC TCG GCT TCG GCT CTT AG-3′. The upstream and downstream primers for FOXO1-(256–655) were 5′-GGA GAA GAG CTG GAT CCA TGG ACA ACA AC-3′ and 5′-CGG GCC CTC TAG ATC AGC CTG ACA CC-3′, respectively.

To generate FLAG-FOXO1(ΔFK), the N-terminal 0.471-kb fragment was generated by PCR using primers 5′-GAC GGA TCC ATG GCC GAG GCG CCT CAG GTG GT-3′ and 5′-CAA GAT ATC GCG GCG GGA CGA GCT GCT CTT GC-3′ and subcloned into the BamHI and EcoRV sites of pCMV-3×FLAG-IA (Stratagene), and the C-terminal 1.193-kb fragment was generated with primers 5′-CGA GAT ATC AAC AAC AGT AAA TTT GCT AAG AGC C-3′ and 5′-CGT CTC GAG TCA GCC TGA CAC CCA GCT ATG TGT-3′ and cloned into the EcoRV and XhoI sites. The vector encodes recombinant FOXO1 protein that misses the 101 amino acid residues of the Forkhead box (from amino acid 157 to 259).

MDM2 siRNAs were subcloned into pSilencer-Neo (Ambion). The corresponding oligonucleotides for generating the MDM2 siRNA were 5′-GAT CCG CAG GTG TCA CCT TGA AGG TTT CAA GAG AAC CTT CAA GGT GAC ACC TGT TTT TTG GAA A-3′ and 5′-GAT CCG TGG TTG CAT TGT CCA TGG CTT CAA GAG AGC CAT GGA CAA TGC AAC CAT TTT TTG GAA A-3′. Oligonucleotides for green fluorescence protein (GFP) siRNA were from Ambion.

Transfections and Immunological Assays—For co-precipitation analyses, 1×10^6 cells were plated in 100-mm dishes in medium containing 10% fetal bovine serum. One day after plating, cells were transfected with the indicated plasmids by Lipofectamine Plus following the protocol from Invitrogen. Cellular extracts were prepared in a buffer containing 20 mM Tris-HCl (pH 7.5), 0.5% Nonidet P-40, 250 mM NaCl, 3 mM EDTA, 3 mM EGTA, 10 μg/ml aprotinin, 10 μg/ml leupeptin, 10 mM benzamidine, and 1 mM phenylmethylsulfonyl fluoride. After preclearance by incubating with protein A-agarose for 1 h, followed by brief centrifugation, the extracts were incubated sequentially with 1–3 μg of antibody and protein G-agarose beads for 4 h at 4 °C. After four washes with the lysis buffer, the immunoprecipitates were eluted from the beads by boiling in SDS-PAGE loading buffer.

For immunoblotting, cellular extracts or immunoprecipitates were separated on SDS-PAGE, transferred to a nitrocellulose membrane, probed with the cognate antibody, and visualized with enhanced chemiluminescence with the ECL kit from Amersham Biosciences.

FIGURE 1. **MDM2 promotes the degradation of FOXO in a proteasome-dependent manner.** *A*, inverse correlation between MDM2 and FOXO3A protein expression in different cancer cell lines and MEFs. Cellular extracts were subjected to immunoblotting with anti-FOXO3A antibody (H-144). The membrane was washed and reprobed with anti-MDM2 (SMP-14). *B*, inverse correlation between MDM2 and FOXO in p53 null and p53 and MDM2 double null MEFs. Cellular extracts were subjected to immunoblotting with antibodies against FOXO1 (H-128), MDM2 (2A10), FOXO3A (H-144), and β-actin (AC-74), as indicated. *C*, stable expression of MDM2 decreases endogenous FOXO3A. Extracts of H1299 cells stably expressing MDM2 (*MDM2-1* and *MDM2-2*) or empty vector (*Control*) were subjected to immunoblotting with the indicated antibodies. *D*, knockdown of endogenous MDM2 by siRNA increases the level of endogenous FOXO3A protein. H1299/V138 cells were transfected with 2 μg of siRNA against GFP or MDM2 (*MDM2-s1* and *MDM2-s2*). Cellular extracts were prepared and subjected to immunoblotting with the indicated antibodies. *E*, knockdown of endogenous MDM2 by shRNA increases the level of ectopic FOXO1 protein. H1299/V138 cells were transfected with 0.5 μg of FLAG-FOXO1 together with 2 μg of shRNA vectors against MDM2 (*MDM2-shRNA*) or β-tubulin (*Control-shRNA*). Cellular extracts were prepared and subjected to immunoblotting with the indicated antibodies. *F*, ectopic MDM2 decreases the level of cotransfected FOXO1 protein, which is relieved by MG132. DU145 cells were transfected with 0.8 μg of FLAG-FOXO1 and 1.5 μg of MDM2. 24 h posttransfection, cells were incubated with or without MG132 for 6 h. Cellular extracts were subjected to immunoblotting (*IB*) with indicated antibodies. *G*, overexpression of MDM2 decreases the half-life of FOXO1 protein. H1299 cells were transfected with 0.8 μg of FLAG-FOXO1 and 1.5 μg of control vector, full-length (MDM2), or C-terminal truncated MDM2 (*MDM2(1–361)*). 24 h post-transfection, cells were treated with cycloheximide (*CHX*) for the indicated length of time. Cellular extracts containing equal amount of proteins were subjected to immunoblotting (*lower panels*). The immunoblotting signals were quantified by computer-based density scanning. The FOXO1 signals were normalized with cognate β-actin signals and plotted (*graph*).

For immunofluorescence analyses, H1299 cells, MEFs, or transfected cells on coverslips were cultured in Dulbecco's modified Eagle's medium containing 0.5% fetal bovine serum for 16 h, washed once with phosphate-buffered saline (PBS), and fixed in 4% paraformaldehyde for 10 min at 37 °C. The cells were permeabilized at room temperature for 30 min in buffer containing 1% Triton X-100 and 1% bovine serum albumin and incubated in PBS containing 0.2% Nonidet P-40, 1% bovine serum albumin, and primary antibody for 1 h. After washing three times in PBS, cells were incubated for 45 min with goat anti-mouse IgG conjugated with Alexa Fluor 594-conjugated (red) or fluorescein isothiocyanate-conjugated (green) anti-rabbit IgG (Molecular Probes), followed by three washes with PBS. The slides were dried and mounted with Vectashield mounting medium containing 4′,6′-diamidino-2-phenylindole (DAPI) for nuclear staining. Regular fluorescent microscopic images were obtained with a Nikon Diaphot microscope and a Photometrix PXL cooled CCD camera. The microscope was equipped with filters for three-color imaging and a motorized stage for obtaining *z*-series images. Digital image files were processed and deconvolved using Oncor Image software (Oncor Inc.). High resolution images of the deconvolved and three-dimensional reconstructed image *z*-series stacks were processed for presentation with Adobe Photoshop. For confocal analyses, samples were viewed with a Leica DMI6000 inverted microscope with TCS SP5 confocal scanner and a ×100, numerical aperture 1.40 plan apochromat oil immersion objective (Leica Microsystems). 405-Diode and HeNe 594 laser lines were used for excitation and tunable filters to minimize interference between fluorochromes. Differential interference contrast imaging was performed using an argon laser line. Scale bars were created with the LAS AF software version 1.6.0 build 1016 (Leica Microsystems).

Ni^{2+}-Nitrilotriacetic Acid (NTA) Pull-down Assay—H1299 cells or MEFs were plated in 100-mm dishes and transfected with 4 μg of His_6-ubiquitin plasmid, 4 μg of FOXO vectors, and 4 μg of MDM2 vectors using Lipofectamine Plus. 24 h post-transfection, cells were harvested and separated into two aliquots: one aliquot (10%) for immunoblotting of transfected proteins and the other (90%) for purification by Ni^{2+}-NTA beads. Cell pellets were lysed in buffer containing 0.01 M Tris-Cl (pH 8), 6 M guanidinium HCl, 0.1 M sodium phosphate, 5 mM imidazole, 10 mM β-mercaptoethanol and were incubated with Ni^{2+}-NTA beads (Qiagen) overnight at room temperature. The beads were washed sequentially with the lysis buffer, a buffer containing 0.01 M Tris-Cl (pH 8), 8 M urea, 0.1 M sodium phosphate, 10 mM β-mercaptoethanol, and a buffer containing 0.01 M Tris-Cl (pH 6.3), 8 M urea, 0.1 M sodium phosphate, 10 mM β-mercaptoethanol. Proteins were eluted with a buffer containing 0.15 M Tris-Cl (pH 6.7), 5% SDS, 200 mM imidazole, 30% glycerol, 0.72 M β-mercaptoethanol and immunoblotted for ubiquitin-conjugated FOXO proteins.

In Vitro Transcription-coupled Translations and Glutathione S-Transferase (GST) Pull-down Assays—FOXO1 protein was produced with pcDNA3-FLAG-FOXO1 as a template using the T7 polymerase-based *in vitro* transcription-coupled translations (Promega, Madison, WI). GST-MDM2 plasmids were transformed into *Escherichia coli* and cultured at 37 °C until the optical density at 600 nm reached 0.6. Then 0.2 mM isopropyl 1-thio-β-D-galactopyranoside was added, and incubations were carried out for another 5 h at 30 °C. Bacterial cultures were lysed by sonication in buffer containing 50 mM Tris (pH 8.0), 10 mM NaCl, 1 mM EDTA, 6 mM $MgCl_2$, 1 mM dithiothreitol, and 1 mM phenylmethylsulfonyl fluoride. GST pull-down analyses were performed using the MagneGST pull-down system (Promega, Madison, WI) according to the vendor's protocol.

In Vitro Ubiquitination Assays—Full-length GST-MDM2 and GST-MDM2-NT-(1–150) were expressed in *E. coli* and bound to glutathione-agarose beads. The substrate FOXO1 was produced by *in vitro* transcription-coupled translation in rabbit reticulocyte lysate using the TNT system (Promega) in the presence of [^{35}S]methionine. 4 μg of GST fusion proteins and 8 μl of the FOXO1 *in vitro* translation product were incubated together to allow the enzyme-substrate interaction to occur. After three washes with PBS containing 0.2% Nonidet P-40, the bead-bound enzyme-substrate complex was incubated at 37 °C for 1 h with 250 ng of GST-Ubc5Hb (Boston Biochem), 250 ng of purified rabbit ubiquitin E1 (Boston Biochem), and 2 μg of His_6-ubiquitin (Boston Biochem) in 20 μl of reaction buffer containing 50 mM Tris (pH 7.5), 2.5 mM $MgCl_2$, 15 mM KCl, 1 mM dithiothreitol, 0.01% Triton X-100, 1% glycerol, 8 mM ATP. The reactions were terminated by boiling in SDS sample buffer and separated by SDS-PAGE. The gel was dried, and the ubiquitin-conjugated FOXO1 proteins were detected by autoradiography.

Apoptotic Analyses and Flow Cytometry—The determination of the survival and apoptotic index of GFP-transfected cells has been described (42). In brief, transfected cells were washed with PBS, fixed in 4% formaldehyde, and stained with DAPI. Representative micrographs were captured by a charge-coupled device camera with a Smart Capture Program (Vysis, Downers Grove, IL) attached to a Leitz Orthoplan 2 fluorescence microscope. The viability of transfected cells in each well was determined by counting the total number of green cells in each well. The apoptotic index of GFP-positive cells was determined by scoring 300 GFP-positive cells for chromatin condensation and apoptotic body formation.

To measure the apoptotic index induced by FOXO1, H1299 cells in 100-mm dishes were transfected with GFP and FOXO1 with or without MDM2. Transfected cells were collected in PBS containing 2.5 mM EDTA; washed twice with cold PBS; resuspended in 1× binding buffer containing 0.01 M Hepes (pH 7.4), 0.14 M NaCl, 2.5 mM $CaCl_2$ at a concentration of 1×10^6 cells/ml; and stained with Annexin-V allophycocyanin and 7-aminoactinomycin D. Cell sorting and flow cytometry analysis were performed on a FACScan (BD Biosciences).

RESULTS

MDM2 Promotes the Degradation of FOXO Factors—While investigating the functional cross-talk between p53 and FOXO signaling pathways, we noticed an inverse correlation between the expression of FOXO3A and the p53 target gene *MDM2* among a panel of human cancer cell lines, including osteosarcoma (Saos2), prostate (LNCaP, PC3, DU145, and JCA1), breast (MCF-7), cervical (HeLa), and

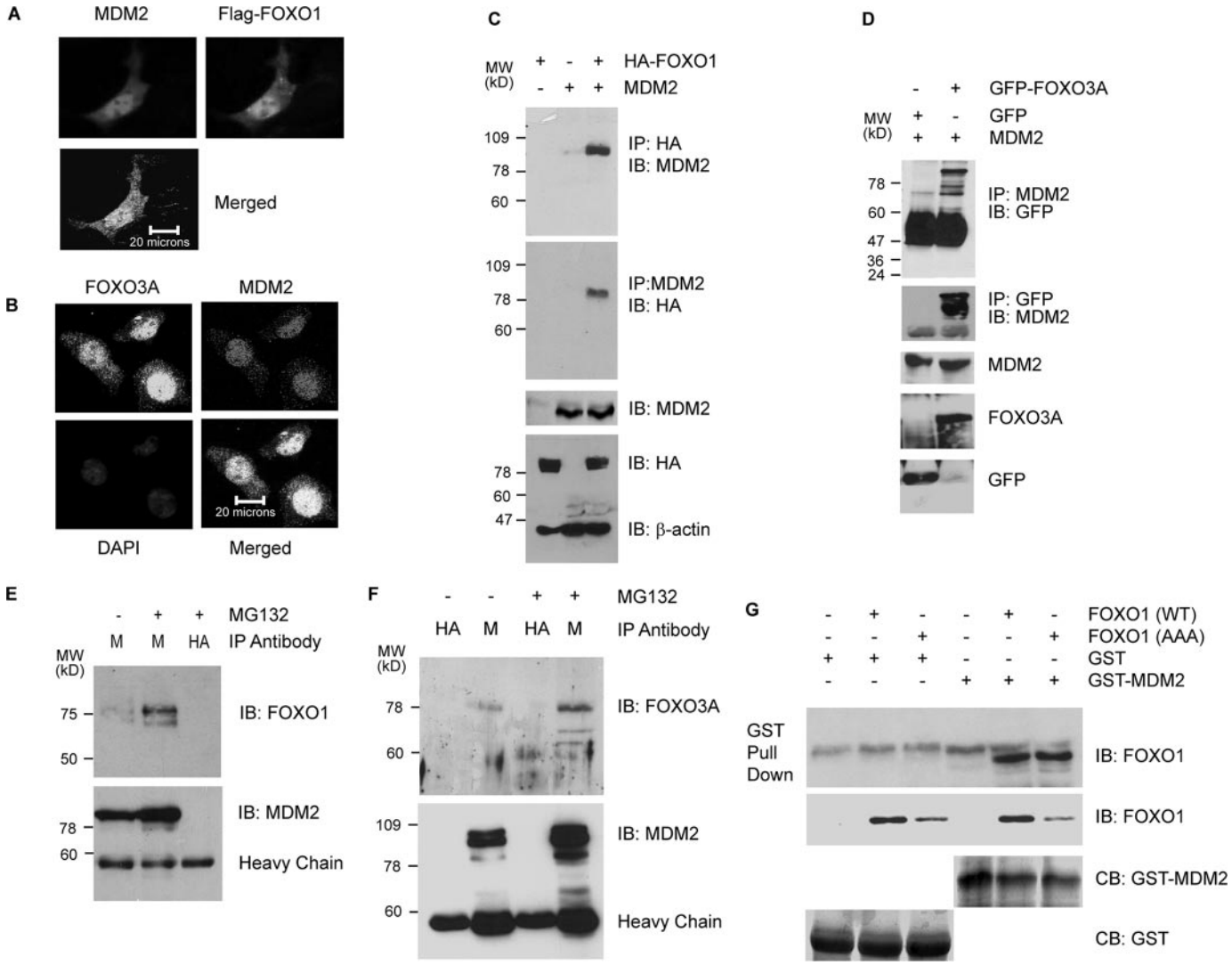

FIGURE 2. **MDM2 interacts with FOXO1 and FOXO3A *in vivo* and *in vitro*.** *A*, colocalization of ectopic MDM2 and FLAG-FOXO1 in p53 and MDM2 double null MEFs. The fibroblasts were transfected with 0.5 μg of FLAG-FOXO1 and 0.5 μg of MDM2 and fixed. The colocalization was determined by immunofluorescence staining with anti-MDM2 and M2 anti-FLAG antibodies and visualized by deconvolution imaging. *B*, colocalization of endogenous MDM2 and FOXO3A. H1299 cells were fixed and subjected to immunofluorescence staining with DAPI, anti-MDM2, and anti-FOXO3A, as indicated. The colocalization was visualized by confocal imaging. *C*, interaction between ectopic FOXO1 and MDM2. H1299 cells were transfected with 2 μg of HA-FOXO1, 2 μg of MDM2, or both. 24 h posttransfection, cellular extracts were prepared and subjected to co-precipitations (*IP*) and immunoblotting (*IB*) with the indicated antibodies. *D*, interaction of ectopic FOXO3A and MDM2. H1299 cells were transfected with 2 μg of MDM2 and 2 μg of GFP or GFP-FOXO3A. 24 h posttransfection, cellular extracts were prepared and subjected to co-precipitations and immunoblotting with the indicated antibodies. *E*, interaction of endogenous MDM2 and FOXO1 in HI299/V138 cells. HI299/V138 cells were cultured at a permissive temperature (32 °C) overnight and treated with vehicle (DMSO) or MG132 for 6 h. Cellular extracts were subjected to co-immunoprecipitations, followed by immunoblotting with the indicated antibodies. *M*, anti-MDM2; *HA*, anti-HA (control). *F*, interaction of endogenous MDM2 and FOXO3A. HEK293T cells in a 100-mm dish were treated with DMSO or MG132 for 6 h. Then cellular extracts were prepared and subjected to co-immunoprecipitations, followed by immunoblotting with the indicated antibodies. *M*, anti-MDM2; *HA*, anti-HA (control). *G*, *in vitro* interaction between FOXO1 and MDM2. FOXO1 produced in *in vitro* transcription-coupled translation reactions was incubated with either GST or GST-MDM2 fusion proteins. Pull-down assays were performed with magnetic glutathione beads, followed by immunoblotting with anti-FOXO1 antibody. The amount of GST and GST-MDM2 proteins used in the pull-down assays was visualized by Coomassie Blue staining after SDS-PAGE (*bottom*).

lung (H1299, H1299/V138) cancer cells (Fig. 1*A*). To determine whether the inverse correlation among cancer cells reflects a negative effect of MDM2 on FOXO protein, the level of FOXO3A and FOXO1 protein expression in p53 null and p53/MDM2 double null MEFs was measured by immunoblotting. As shown in Fig. 1*B*, knocking out MDM2 in MEFs increased the expression of endogenous FOXO1 and FOXO3A proteins. Consistent with the data from MEFs, the stable expression of MDM2 in H1299 cells reduced (Fig. 1*C*) whereas the knockdown of endogenous MDM2 increased (Fig. 1*D*) the expression of endogenous FOXO3A. Unlike MEFs, H1299/V138 cells express low levels of endogenous FOXO1, which are difficult to detect. Thus, we tested the effect of MDM2 silencing on the expression of ectopic FOXO1. As shown in Fig. 1*E*, the knockdown of MDM2 increased the level of ectopic FLAG-FOXO1 expression.

Since MDM2 is an E3 ubiquitin ligase that promotes the proteasome mediated degradation of p53 (43) and of other proteins (33), it is likely that MDM2 decreases the expression of FOXO factors through a similar mechanism. In transient transfection studies, we found that co-expression of MDM2 reduced the expression of FLAG-FOXO1 in DU145 prostate cancer cells, a

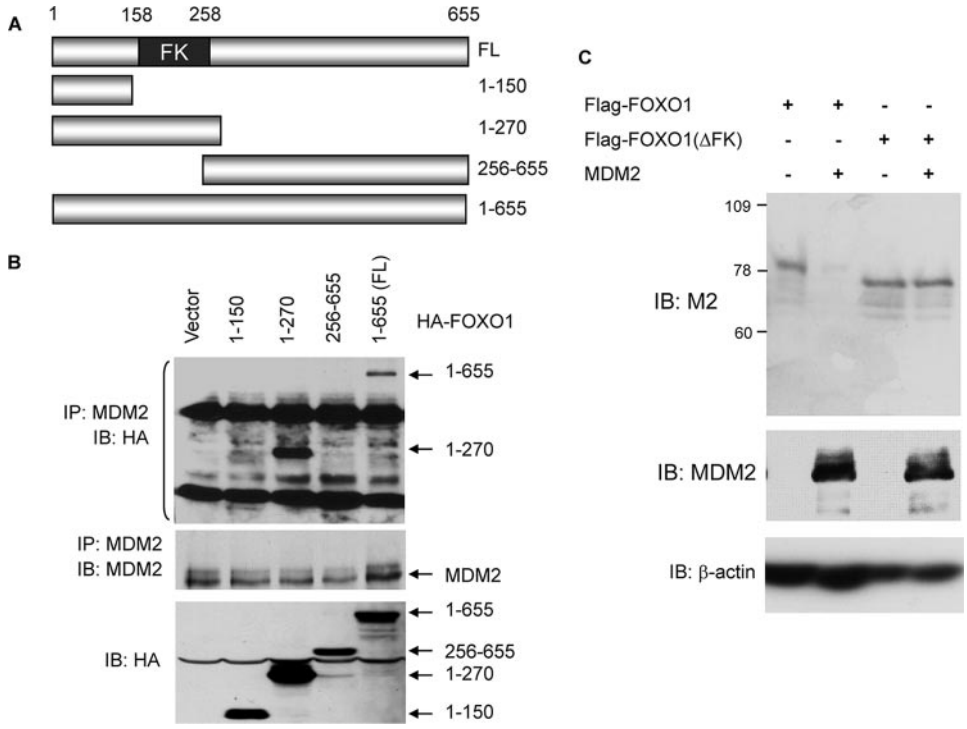

FIGURE 3. **The forkhead box of FOXO1 is required for MDM2 binding.** *A*, diagram of the different HA-FOXO1 deletion constructs used in the interaction studies. *FL*, full-length FOXO1. *B*, co-immunoprecipitation (*IP*) analyses. H1299 cells were transfected with MDM2 and the indicated HA-FOXO1 vectors. Cellular extracts (*lower panel*) or anti-MDM2 immunoprecipitates (*upper panels*) were subjected to immunoblotting (*IB*) with the indicated antibodies. *C*, PC3 cells were transfected with 2 μg of FLAG-FOXO1 or FLAG-FOXO1 deleted of the forkhead box (FOXO1ΔFK) together with 2 μg of control vector or MDM2. Cellular extracts were subjected to immunoblotting with the indicated antibodies. The FOXO(ΔFK) expressed at a higher level than wild type, and reduced amounts of cellular extracts were used as indicated by lower level of β-actin.

process that was prevented by co-treatment with proteasome inhibitor MG132 at two different concentrations (Fig. 1*F*).

To test whether the decreased FOXO protein expression by MDM2 is due to protein degradation, the half-life of FLAG-FOXO1 was measured in H1299 cells cotransfected with control vector, full-length MDM2, or MDM2 mutant (residues 1–361) that lacks the C-terminal ring domain important for its E3 ligase activity. As shown in Fig. 1*G*, the half-life of FOXO1 was decreased by full-length MDM2 from 6 to 3 h relative to the control vector. Moreover, cotransfection with MDM2-(1–361) caused a significant increase in the half-life of the FLAG-FOXO1, possibly due to a dominant negative effect. Overall, these data raise the possibility that MDM2 functions as an E3 ubiquitin ligase for mammalian FOXO factors.

MDM2 Interacts with FOXO Factors in Vivo and in Vitro—Ubiquitin E3 ligases are known to make direct contact with their substrates. Therefore, we investigated whether MDM2 and FOXO factors form a complex in cells. Deconvolution imaging analyses detected ectopic MDM2 and FOXO1 proteins in both the cytoplasm and nucleus of p53 and MDM2 double null MEFs, but co-localization was detected predominantly in the nucleus (Fig. 2*A*). Similarly, confocal imaging gave the same result for endogenous MDM2 and FOXO3A in H1299 cells (Fig. 2*B*).

To determine whether MDM2 and FOXO1 interact in mammalian cells, they were ectopically expressed in H1299 cells, and reciprocal co-immunoprecipitations were performed. As shown in Fig. 2*C*, MDM2 and FOXO1 were co-precipitated in cells that express both proteins. In cells that express either MDM2 or FOXO1, little or no co-precipitation occurred, showing that the co-precipitations were not due to cross-reactivity of the antibodies. Similar analysis showed that MDM2 and GFP-FOXO3A were specifically co-precipitated (Fig. 2*D*).

To test further whether endogenous MDM2 and FOXO1 proteins in mammalian cells interact, H1299/V138 cells expressing a temperature-sensitive p53 mutant (34) were shifted to a permissive temperature for 16 h to induce MDM2 expression and treated with MG132. Cellular extracts were subjected to co-immunoprecipitations with anti-MDM2 antibody or anti-HA antibody as control. As shown in Fig. 2*E*, FOXO1 was precipitated by anti-MDM2 antibody but not by the control antibody, showing that the co-precipitations were not due to antibody cross-reactivity. MG132 treatment increased the level of MDM2 and FOXO expression as well as their co-precipitations. Similar co-precipitation analyses in HEK293T cells treated with MG132 showed that the FOXO3A protein was co-precipitated with MDM2 by anti-MDM2 but not anti-HA antibody and that treatment with MG132 increased the level of MDM2 and FOXO3A expression as well as their co-precipitations (Fig. 2*F*). These studies show that the co-precipitations occur with both endogenous and ectopically expressed proteins.

To determine whether MDM2 and FOXO1 interact *in vitro*, GST and GST-MDM2 fusion proteins were produced in bacteria, bound to glutathione beads, and incubated with FOXO1 proteins produced by *in vitro* transcription-coupled translations. In these GST pull-down assays, wild type FOXO1 was precipitated with GST-MDM2 but not with GST (Fig. 2*G*). A mutant form of FOXO1, FOXO1 (AAA), in which all three AKT phosphorylation sites were mutated to alanine, was also precipitated with GST-MDM2 but not with GST (Fig. 2*G*). This experiment shows that FOXO1 and MDM2 form a complex *in vitro*, and the complex formation occurs independently of the phosphorylation of FOXO1 by AKT.

The Interaction between MDM2 and FOXO1 Is Mediated by the Forkhead Box of FOXO1 and the Region of MDM2 That Controls Nuclear-Cytoplasmic Shuttling—To define the region in FOXO1 necessary for binding to MDM2, H1299 cells were transfected with MDM2 together with full-length FOXO1 or its deletion constructs fused to the HA tag (Fig. 3*A*), and cellular extracts were then co-immunoprecipitated with an anti-MDM2 antibody. As shown in Fig. 3*B*, the full-length FOXO1

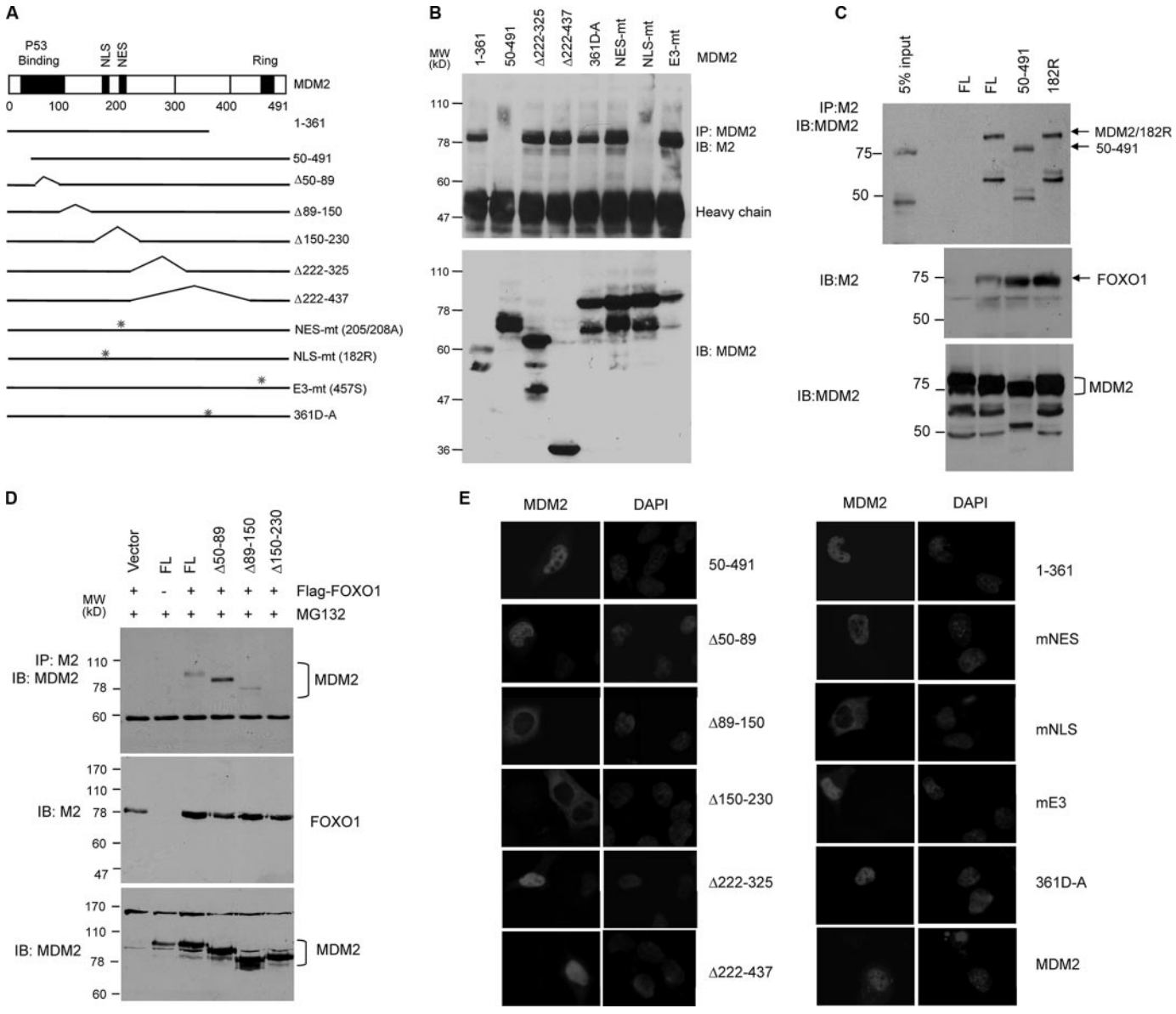

FIGURE 4. **The MDM2 sequence involved in the interaction with FOXO1 is defined to the region that contains nuclear localization and export sequences.** *A*, a diagram showing different MDM2 mutant constructs used in the interaction studies. *B*, co-immunoprecipitations in the absence of proteasome inhibitors. H1299 cells were transfected with 2 μg of FLAG-FOXO1 and 2 μg of MDM2 mutants. Anti-MDM2 immunoprecipitates (*upper panels*) or cellular extracts (*lower panel*) were subjected to immunoblotting with the indicated antibodies. *C* and *D*, co-immunoprecipitation in the presence of MG132. H1299 cells were transfected with 2 μg of FLAG-FOXO1 and 2.5 μg of the MDM2 mutants and treated with MG132 for 6 h. Cellular extracts or anti-FLAG precipitates were subjected to immunoblotting with indicated antibodies. *E*, cellular localization of MDM2 mutants. H1299 cells were transfected with the indicated MDM2 constructs and immunostained with a MDM2 antibody. DAPI staining shows the nucleus.

protein was co-precipitated with MDM2. Deletion of the C-terminal region of FOXO1 did not alter the co-precipitations. However, further deletion into the forkhead box abolished the interaction, suggesting that the forkhead box is necessary for the interaction. Consistent with this interpretation, the expression of FOXO1 protein deleted of the forkhead box was no longer decreased by MDM2 (Fig. 3*C*). The FOXO(ΔFK) expressed at a much higher level than wild type, presumably due to increased protein stability. It remains to be determined whether the forkhead box alone is sufficient for the interaction, since in our cell system, the construct that contains only the forkhead box of FOXO1 did not express adequate amounts of the protein, presumably due to its instability.

To define the MDM2 region responsible for FOXO1 binding, different MDM2 constructs (Fig. 4*A*) were transfected with FLAG-FOXO1 into H1299 cells. Cellular extracts were immunoprecipitated with MDM2 antibody, and the co-precipitated FOXO1 was detected by anti-FLAG antibody. As shown in Fig. 4*B*, all MDM2 mutants, except MDM2-(50–491) (p53 binding-deficient) and MDM2 NLS-mt (182R, nuclear localization sequence-defective), interacted with FOXO1. However, in the presence of the proteasome inhibitor MG132, both MDM2-(50–491) and MDM2 NLS-mt were co-precipitated with FLAG-FOXO1 using the same anti-FLAG antibody (Fig. 4*C*). The reason for their lack of interaction with FOXO1 in the absence of MG132 is unclear, but it is likely to be caused by proteasome degrada-

tion of the protein complex. Direct immunoblotting showed that all MDM2 mutants were expressed at significant levels, and most MDM2 proteins were detected in multiple forms, presumably due to cleavages by proteases (44).

Further co-precipitation analyses with more MDM2 mutants in the presence of MG132 showed that deletion of amino acids 150–230 abrogated FOXO1 binding (Fig. 4*D*). Consistent with the fact that this region contains the nuclear localization sequence, the deletion mutant is mainly localized to cytoplasm (Fig. 4*E*). However, cytoplasmic localization is clearly not the reason for its lack of interaction with FOXO1, because under the same conditions, nuclear localization sequence mutant (MDM2 NLS-mt) was able to interact with FOXO1 (Fig. 4*C*). In addition to cellular localization sequences, the 150–230 region is also part of an inhibitory domain that suppresses cell cycle progression independently of p53 (45). It is also involved in interactions with several proteins, including TBP and p300 (45).

MDM2 Promotes the Ubiquitination of FOXO1 and FOXO3A Proteins—To test whether MDM2 promotes the ubiquitination of FOXO factors, H1299 cells were transfected with wild type FLAG-FOXO1 or with FOXO1 mutant in which all three AKT phosphorylation sites were changed to alanines (15). The effect of ectopic MDM2 on FOXO1 ubiquitination by co-transfected Myc-tagged ubiquitin was measured in anti-FLAG precipitates (Fig. 5*A*). In the absence of ectopic MDM2, little FOXO1 ubiquitination was detected. This result is consistent with the fact that H1299 cells are p53-deficient and contain low levels of endogenous MDM2. The co-transfection of MDM2 increased ubiquitination of the wild type but not of the mutant FOXO1. The data argue that the MDM2 stimulation of FOXO1 ubiquitination requires the phosphorylation of FOXO1 at the AKT sites.

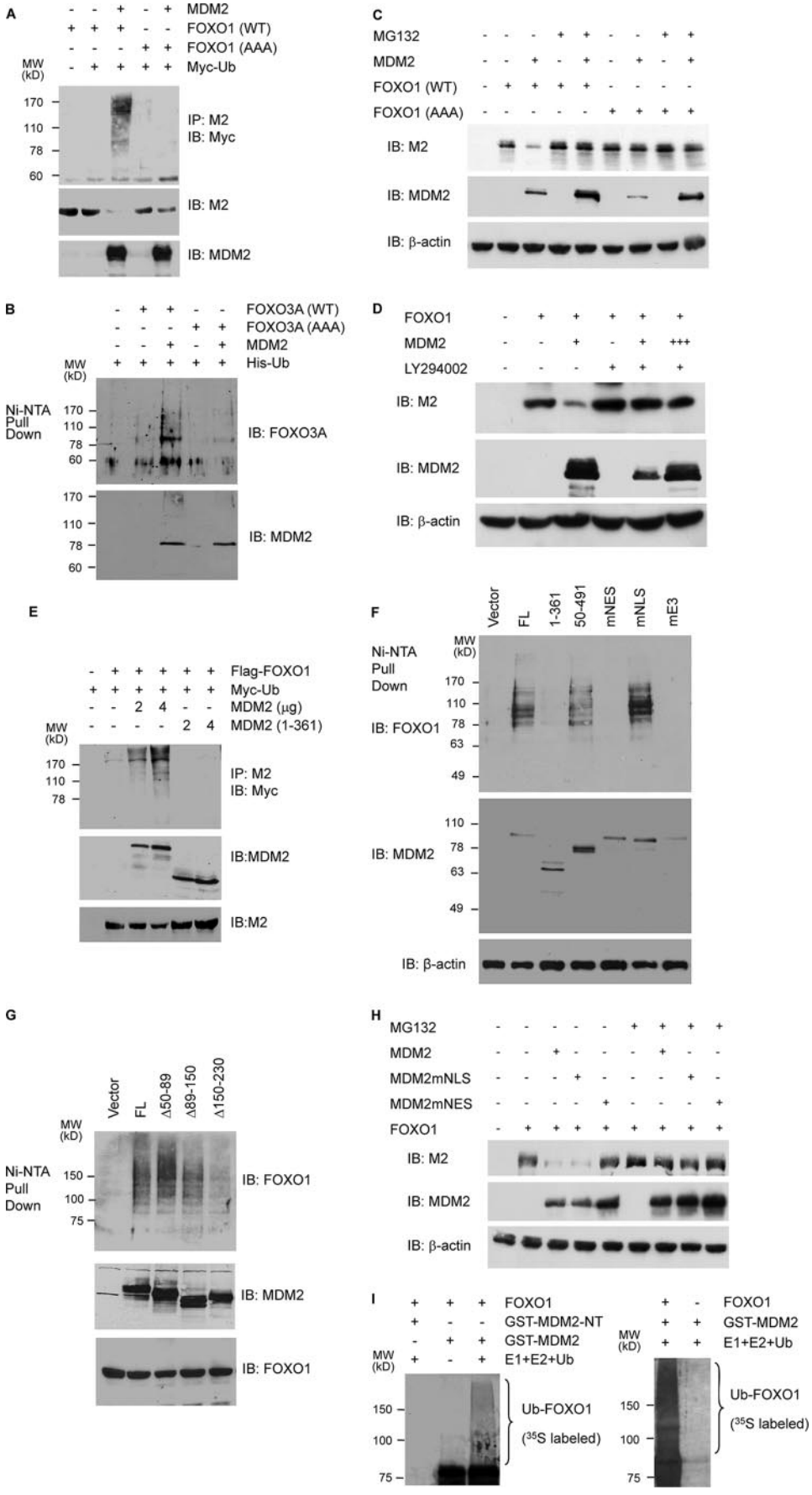

To further test whether the effect of MDM2 extends to other FOXO factors, FOXO3A- and His-tagged ubiquitin were transfected into H1299 cells. The effect of MDM2 on FOXO3A ubiquitination was measured by immunoblotting with anti-HA antibody following nickel bead pull-down under denaturing conditions. As shown in Fig. 5*B*, MDM2 increased FOXO3A ubiquitination in a manner dependent on the phosphorylation at the AKT sites. These data suggest that the MDM2 stimulation of ubiquitination is not restricted to FOXO1.

In agreement with the AKT site dependence of the MDM2 effect on FOXO ubiquitination, MDM2 did not stimulate the proteasome degradation of FOXO1 mutant in which all three AKT phosphorylation sites were changed to alanines (Fig. 5*C*). Furthermore, LY294002, an inhibitor of phosphatidylinositol 3-kinase/AKT signal pathway, diminished the ability of MDM2 to decrease FOXO1 protein expression (Fig. 5*D*). It is important to note that LY294002 decreased ectopic MDM2 expression and that increased amounts of MDM2 plasmids were used to produce MDM2 protein close to the level detected in the absence of LY294002. The data show that the MDM2 stimulation of FOXO1 degradation needs the AKT-mediated phosphorylation.

In p53 and MDM2 double null MEFs, wild type MDM2 stimulated the ubiquitination of FOXO1 in a dose-dependent manner, whereas the MDM2 mutant, in which the C-terminal RING domain is deleted, had no effect (Fig. 5*E*), suggesting a potential involvement of the E3 ligase activity. Nickel bead pull-down assays under denaturing conditions revealed that MDM2 mutant, the mE3 (or 457S), having a point mutation in the RING domain, did not stimulate FOXO1 ubiquitination (Fig. 5*F*), confirming that FOXO1 ubiquitination by MDM2 requires its ubiquitin ligase activity. Interestingly, a constitutively nuclear MDM2 in which the nuclear export sequence was mutated, the mNES, did not promote FOXO1 ubiquitination (Fig. 5*F*), although it contains intact RING domain and interacts with FOXO1 (Fig. 4*B*). On the other hand, two cytoplasmic MDM2 mutants, MDM2 mNLS and MDM2 (Δ89–150), stimulated FOXO1 ubiquitination (Fig. 5, *F* and *G*), showing that the ubiquitination of FOXO1 by MDM2 is likely to occur in the cytoplasm. MDM2 mutant (Δ150–230), which was confined to the cytoplasm (Fig. 4*E*) and did not interact with FOXO1 (Fig. 4*D*), was unable to stimulate FOXO1 ubiquitination, suggesting that ubiquitination requires FOXO1 interaction. Overall, the data suggest that FOXO1 interacts with MDM2 in both the nucleus and the cytoplasm, but the ubiquitination and degradation by MDM2 requires that the interaction takes place in the cytoplasm. Consistent with this interpretation, the NLS mutant MDM2 stimulated the proteasome degradation of FOXO1 protein in a way similar to wild type but, the nuclear export sequence mutant did not show this activity in parallel analyses (Fig. 5*H*).

To fully establish MDM2 as an E3 ligase for FOXO1 ubiquitination, we tested the ability of recombinant MDM2 to catalyze the ubiquitination of FOXO1 *in vitro*. In this assay, GST-MDM2 stimulated the ubiquitination of *in vitro* translated FOXO1 in the presence of purified E1, ubiquitin-conjugating enzyme, and ubiquitin (Fig. 5*I*, *top*). GST fused to an MDM2 N-terminal fragment had no effect on the ubiquitination of FOXO1. In reactions performed with a transcription-coupled translation product from a control vector, the majority of the ^{35}S-labeled ubiquitin conjugates disappeared, showing that they were FOXO1 proteins (Fig. 5*I*, *bottom*). In combination with the binding data and whole cell ubiquitinations with MDM2 mutants, the *in vitro* data demonstrated that MDM2 functions as an ubiquitin E3 ligase for FOXO proteins.

MDM2 Suppresses the Expression of FOXO Target Genes and Protects the Cells from FOXO1-induced Apoptosis—TRAIL, p27 CDK inhibitor, and manganese superoxide dismutase are FOXO target genes that mediate the effect of FOXO proteins on cell cycle arrest, apoptosis, and detoxification of reactive oxygen species. Their transcription products are directly regulated by FOXO factors. Consistent with the ubiquitination and degradation of FOXO factors by MDM2, stable expression of MDM2 in H1299 cells decreased p27 and manganese superoxide dismutase expression levels (Fig. 6*A*). Knockdown of MDM2 increased the expression of TRAIL (Fig. 6*B*).

To test whether MDM2 protects cells from FOXO-induced apoptosis, H1299 cells were transiently transfected with GFP and either control vector, FOXO1, or FOXO1 in combination with MDM2. The survival of the transfected cells was measured. The expression of FOXO1 decreased the number of transfected (green) cells, an effect that was relieved by MDM2 co-expression (Fig. 6*C*). To confirm that the change in the viability of transfected cells is the result of cell apoptosis, transfected

FIGURE 5. **MDM2 promotes the ubiquitination and degradation of FOXOs in a manner dependent on AKT-mediated phosphorylations and cytoplasmic localization.** *A*, MDM2 promotes the ubiquitination of FOXO1 *in vivo*. H1299 cells were transfected with the indicated vectors. Cellular extracts were prepared, and FOXO1 ubiquitination was determined by precipitations (*IP*) with M2 anti-FLAG followed by immunoblotting (*IB*) with a Myc antibody (*upper panel*). The level of FOXO1 and MDM2 expression (*lower panels*) was determined by immunoblotting of the cellular extracts. *B*, MDM2 promotes the ubiquitination of FOXO3A *in vivo*. H1299 cells were transfected as indicated. Cellular extracts were subjected to Ni^{2+}-NTA bead pull-down assays followed by immunoblotting with an HA antibody (*upper panel*). The level of MDM2 expression was determined by immunoblotting of the cellular extracts (*lower panel*). *C*, MDM2 promotes the FOXO1 degradation. H1299 cells were transfected with 2 μg of the indicated plasmids. 24 h later, the cells were treated with either DMSO (−) or 10 μM MG132 for 6 h. Cellular extracts were subjected to immunoblotting with the indicated antibodies. *D*, effect of LY294002 on the ability of MDM2 to decrease FOXO1 expression. PC3 cells were transfected with 2 μg of FLAG-FOXO1 and 2 (+) and 6 (+++) μg of MDM2. 15 h later, the cells were treated with either DMSO or 10 μM LY294002 for 8 h. Cellular extracts were subjected to immunoblotting with the indicated antibodies. *E*, dose-dependent effect of MDM2 on FOXO1 ubiquitination and the requirement of its carboxyl-terminal RING domain. p53 and MDM2 double null MEFs were transfected with the indicated vectors, and the ubiquitination of FOXO1 and the level of FOXO1 and MDM2 expression were determined by immunoblotting of the cellular extracts. *F* and *G*, ubiquitination of FOXO1 requires MDM2 E3 ligase activity, cytoplasmic localization, and interaction with FOXO1. p53 and MDM2 double null MEFs were transfected with the indicated vectors, and the ubiquitination of FOXO1 as well as the level of FOXO1 and MDM2 expression were determined by immunoblotting of the cellular extracts. *H*, the dependence on cytoplasmic localization for the ability of MDM2 to decrease FOXO1 level. H1299 cells were transfected with 2 μg of FLAG-FOXO1 and MDM2. 24 h later, the cells were treated with either DMSO or 10 μM MG132 for 6 h. *I*, MDM2 promotes FOXO1 polyubiquitination *in vitro*. GST-MDM2 and GST-MDM2-(1–150) (*GST-NT*) were produced in *E. coli* and bound to glutathione-agarose beads, and the ubiquitination of the bound FOXO1 protein was assayed as described under "Materials and Methods." Ubiquitinated FOXO1 was visualized by autoradiography as a high molecular weight smear above the unmodified FOXO1 band.

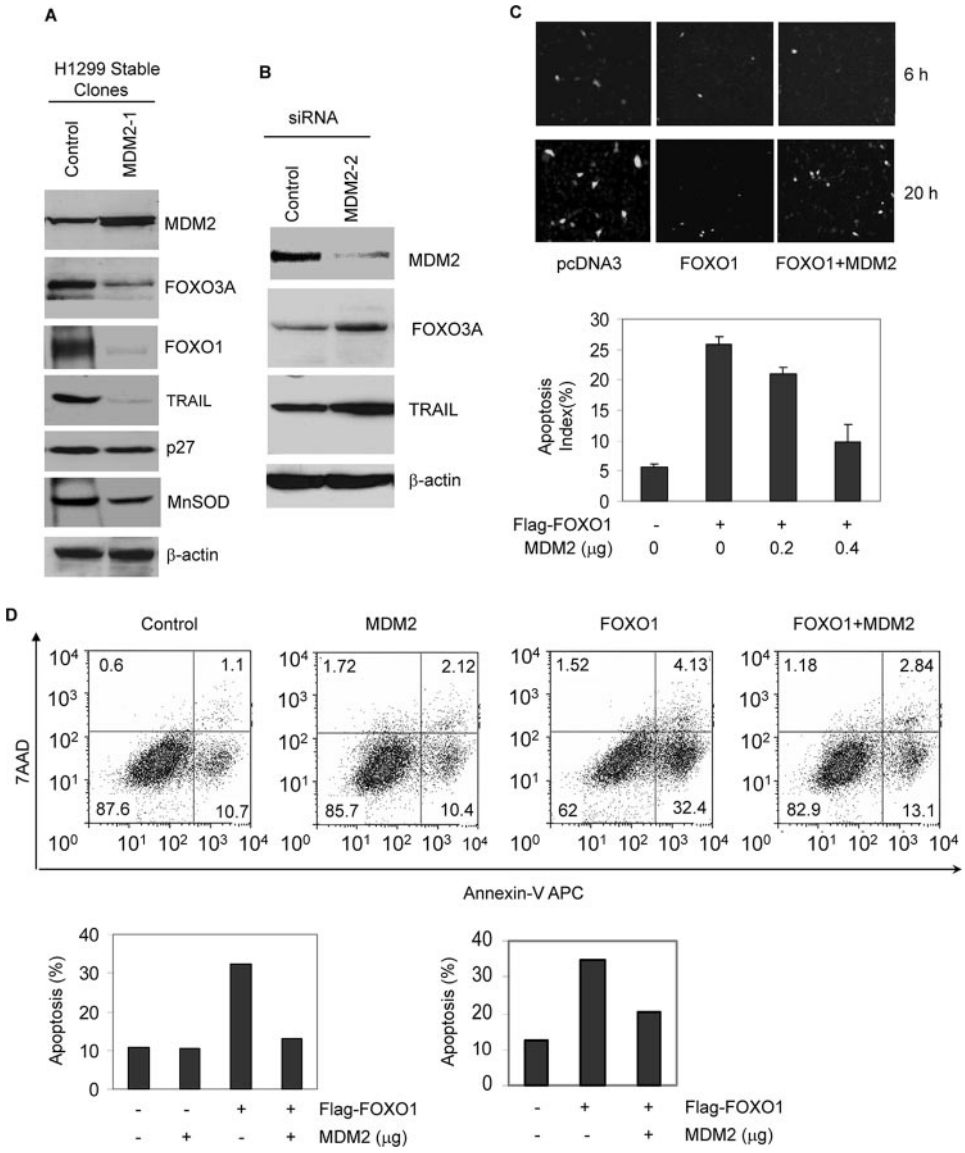

FIGURE 6. **MDM2 suppresses the expression of FOXO1 target gene expression and protects cells from FOXO1 induced apoptosis.** *A*, stable expression of MDM2 suppresses the expression of FOXO target genes. Whole cell extracts of H1299 cells and MDM2 stable clones were subjected to immunoblotting with the indicated antibodies. *B*, MDM2 siRNA enhances the induction of TRAIL by FOXO1. H1299 cells were transfected with siRNA against GFP or MDM2. 48 h posttransfection, cellular extracts were prepared and subjected to immunoblotting with the indicated antibodies. *C*, MDM2 protects cells from FOXO1-induced apoptosis, as measured by manual counting. H1299 cells were transfected with 0.2 μg of pLNCE and 0.5 μg of FLAG-FOXO1 together with or without 1 μg of MDM2. Then the cells were fixed and stained with DAPI. Representative micrographs were captured by a CCD camera attached to a fluorescence microscope (*upper panels*). The apoptotic index of GFP-positive cells was determined by scoring 300 GFP-positive cells for chromatin condensation and nuclear fragmentation. Triplicate samples were analyzed per data point, and the graph represents three independent experiments. *D*, MDM2 protects cells from FOXO1-induced apoptosis, as measured by flow cytometry. H1299 cells were transfected with GFP-spectrin and FLAG-FOXO1 with or without MDM2. Transfected (GFP-positive) cells were separated from nontransfected (GFP-negative) cells by FACS-based sorting. The apoptotic index of GFP-positive cells was determined with the Annexin-V kit. The flow cytometry profile of a representative experiment was shown. Data from two independent analyses are shown as *bar graphs*. *MnSOD*, manganese superoxide dismutase.

cells were fixed and stained with DAPI, and their nuclear morphology was examined for features of apoptosis under a fluorescence microscope that permits the simultaneous visualization of both blue and green fluorescence. The apoptotic index, as determined by scoring apoptotic cells in 300 green cells/sample, was 5% for controls and 25% for cells transfected with FOXO1. Co-expression of MDM2 suppressed the increase in the apoptotic index induced by FOXO1 in a dose-dependent manner (Fig. 6*C*).

The data were confirmed by independent analyses of early apoptosis with the Annexin-V method after FACS-based sorting. As shown in Fig. 6*D*, two independent analyses of cells co-transfected with GFP-spectrin showed that FOXO1 expression increased apoptosis of transfected cells by about 3-fold, which was partially suppressed by the co-transfection of MDM2. The degree of induction by FOXO1 and the suppression by MDM2 varied between experiments, because the basal line of the FACS machine drifted from time to time.

p53 Induces Degradation of FOXO3A in an MDM2-dependent Manner—Since MDM2 is a p53 target gene, we next tested whether p53 acts through MDM2 to regulate the expression of FOXO proteins. H1299/V138 cells that express a temperature-sensitive p53 were shifted to a permissive temperature to allow p53 activation. At different times after p53 activation, the levels of MDM2 and FOXO3A proteins were monitored by immunoblotting (Fig. 7*A*) and showed that MDM2 protein was induced to a maximum level 5 h post-p53 activation, and then FOXO3A and MDM2 gradually decreased. MG132 treatment prevented the time-dependent decrease in the level of the FOXO3A protein (Fig. 7*B*), suggesting that the decrease is due to proteasome-mediated degradation. Knockdown of MDM2 by siRNA partially relieved FOXO3A down-regulation by active p53, supporting the notion that the p53-induced decrease is MDM2-dependent (Fig. 7*C*).

Treatments with UV light are known to regulate the level of p53 protein expression. To test whether p53 induction by UV leads to a change in FOXO protein stability, wild type and p53 null MEFs were challenged with UV. Then the level of FOXO3A protein was measured at different time points after the addition of cycloheximide (Fig. 7*D*). It is apparent that FOXO3A protein is much more stable in p53-null than in wild type MEFs. Overall, the data in Fig. 7 suggest that p53 and FOXO factors may use MDM2 as a common E3 ligase to

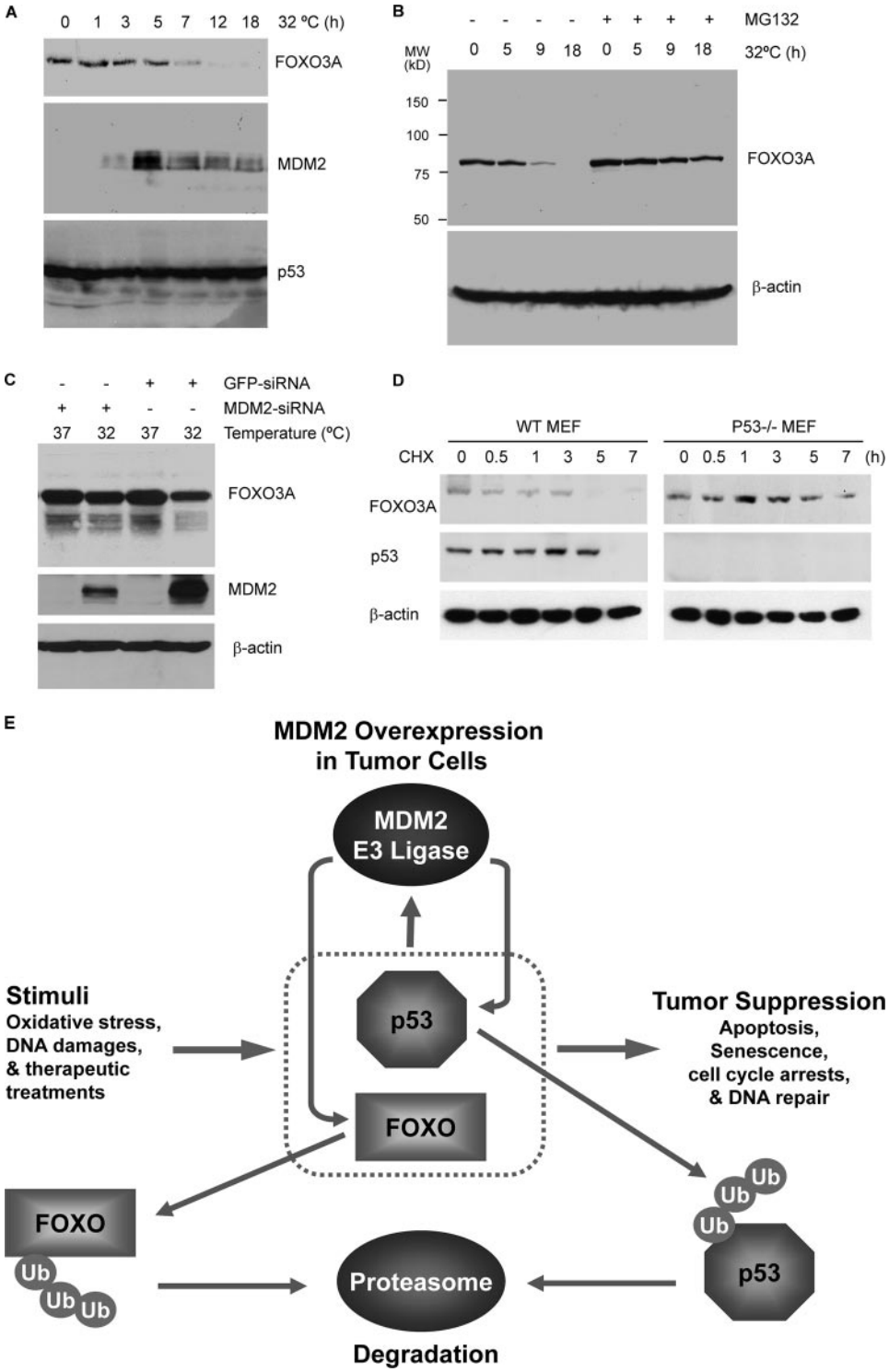

FIGURE 7. **p53 induces the degradation of FOXO3A protein through MDM2.** *A*, p53 expression causes the down-regulation of endogenous FOXO3A protein. H1299/V138 cells at restrictive temperature were shifted to 32 °C for the indicated length of time. Cellular extracts were prepared and subjected to immunoblotting. *B*, MG132 blocks the protein expression decrease of FOXO3A. H1299/V138 cells were shifted to 32 °C as in *A* but treated with MG132 for 6 h before cellular extracts were prepared for immunoblotting. *C*, knockdown of MDM2 partially relieves p53-induced FOXO3A down-regulation. H1299/V138 cells were transfected with scrambled or MDM2 siRNA. 24 h posttransfections, cells were shifted to 32 °C and cultured for 18 h. Then immunoblotting was performed with the indicated antibodies. *D*, effect of p53 on FOXO3a protein stability after UV treatment. Wild-type (*WT*) and p53 null MEFs were treated with UV (0.15 J) and then with 10 μg/ml cycloheximide (*CHX*). The cells were harvested at the indicated time points. Cellular extracts were subjected to immunoblotting for the indicated proteins. *E*, a working model describing how cellular DNA damage response suppresses tumorigenesis through the functions of p53 and FOXO proteins and how MDM2 overexpression in cancer cells promotes tumor growth by inducing the degradation of both p53 and FOXO proteins through the ubiquitin-proteasome pathway. The model also describes the possibility that after DNA repair is accomplished, MDM2 induced by p53 can turn off both p53 and FOXO factors as a feedback mechanism.

regulate their expression as part of the cellular response to DNA damage.

DISCUSSION

As mentioned earlier, mammalian FOXO proteins are ubiquitinated, and their levels are regulated by proteasome-mediated degradation, but a general ubiquitin E3 ligase for FOXO proteins remains to be identified. Skp2 was reported to mediate the ubiquitination and degradation of FOXO1, but such activity appears to be restricted to FOXO1 (46). So far, no mutational analyses and *in vitro* enzyme assays have been performed to show direct involvement of Skp2 E3 activity in FOXO ubiquitination. It remains to be determined whether Skp2 promotes FOXO1 ubiquitination directly, through its intrinsic E3 activity or indirectly through another E3 ligase. The present study identified MDM2 as a general ubiquitin E3 ligase for mammalian FOXO factors. We present multiple lines of evidence to support this conclusion. First, the manipulation of MDM2 expression by genetic deletion, knocking down with siRNA, and either transient or stable overexpression leads to changes in the level of FOXO1 and FOXO3A proteins in the opposite direction. Second, down-regulation of FOXO1 protein by MDM2 is relieved by a proteasome inhibitor, and the half-life of FOXO1 protein is decreased by ectopic MDM2. Third, MDM2 binds to FOXO1 and FOXO3A and promotes their ubiquitination. The latter depends on both the ability of MDM2 to bind FOXO proteins in the cytoplasm and its E3 ligase activity. This is supported by the fact that MDM2 mutant Δ150–230, where the FOXO binding region is deleted, did not stimulate FOXO1 ubiquitination although it contains an intact RING domain. In addition, MDM2 mutants with either deletion (MDM2-(1–361)) or mutation (MDM2 mE3 (457S)) of the C-terminal RING domain lost their ability to stimulate FOXO ubiquitination, although they retained the capacity to interact with FOXO1. Finally, recombinant MDM2 catalyzed the ubiquitination of FOXO1 in test tube reactions, showing a direct substrate-enzyme relationship. It is important to note that two recent independent studies published during the submission of our work showed that MDM2 stimulates FOXO3a polyubiquitination and degradation in breast cancer cells after extracellular signal-regulated kinase phosphorylation (47) and FOXO4 monoubiquitination (48). Collectively, the studies show that MDM2 acts downstream of multiple kinases to control FOXO ubiquitination and activity.

In response to stimulation by interleukin-3, insulin, or platelet-derived growth factor, activated AKT oncogene triggered proteasome-dependent degradation of its substrates, including FOXO1 and FOXO3A (15, 22, 23). Ubiquitination was found to depend on phosphorylations at sites that direct the cytoplasmic localization of FOXO factors by AKT. FOXO1-AAA, in which all three AKT sites are mutated to nonphosphorylatable alanines, bound to MDM2 (Fig. 2*G*), but its level of ubiquitination and expression was not affected by MDM2 (Fig. 5). Similarly, the ubiquitination of the FOXO3A-AAA was also not affected by MDM2. The data suggest that MDM2 acts as a conditional E3 ligase for FOXO proteins, which is functional after FOXO phosphorylations at AKT sites. Previous studies (49, 50) show that phosphorylation of MDM2 by AKT inhibits its interaction with ARF, increases its stability, and promotes its ability to bind and degrade p53. It remains to be determined whether the phosphorylation of MDM2 by active AKT regulates its ability to stimulate FOXO ubiquitination.

Protein ubiquitination and degradation occur in both nucleus and cytoplasm (51). In our analyses, the MDM2 mutant with defective nuclear export sequence but an intact RING domain is able to bind FOXO1 but unable to increase FOXO1 ubiquitination, but the cytoplasmic MDM2, both the MDM2 mNLS and MDM2 (Δ89–150), stimulated the ubiquitination, suggesting that the cytoplasmic localization of MDM2 is required for its function as an E3 ligase for FOXO factors. Considering the data indicating that nuclear FOXO1-AAA is not ubiquitinated by MDM2, it is reasonable to conclude that FOXO ubiquitination occurs in the cytoplasm. However, such a conclusion might appear paradoxical to the immunofluorescence staining finding that the colocalization of MDM2 and FOXO was mainly detected in the nucleus. It is important to point out that the colocalization studies were performed in cells grown in medium containing a low level of serum, which minimizes the AKT activity and inhibits FOXO cytoplasmic localization and degradation. Consistent with the degradation in cytoplasm, the interaction between cytoplasmic MDM2 and FOXO1 was difficult to detect unless the proteasome activity was inhibited by MG132. The fact that the MDM2 mNLS that does not enter the nucleus interacted with FOXO1 and stimulated its ubiquitination suggests that nuclear interaction between MDM2 and FOXO proteins is not required for FOXO ubiquitination, suggesting that the nuclear interaction between FOXO factors and MDM2 exerts an effect on FOXO factors that is separable from degradation. In the case of p53, it has been shown that monoubiquitination by MDM2 promotes its cytoplasmic localization, whereas the polyubiquitination stimulates its degradation in the nucleus (52). FOXO4 has recently been shown to be monoubiquitinated, which increases its transcriptional activity (53). In our studies, a positive effect of MDM2 on the transcriptional activity of FOXO1 was detected in transient transfection reporter assays (data not shown).

Mammalian FOXO factors and p53 are tumor suppressors and aging regulators that function similarly in many ways. They induce apoptosis (5) and cell cycle arrests (2–4) and regulate cellular responses to DNA damage and stress (6, 7) through the transcriptional induction of a similar set of target genes, including the p21 CDK inhibitor, death ligands, GADD45, etc. p53 and MDM2 are known to form a feedback loop, in which p53 induces MDM2 by activating MDM2 transcription, and MDM2 in turn negatively regulates p53 by binding and promoting p53 ubiquitination and degradation (54). The feedback loop keeps the p53 function in check under normal conditions. Upon DNA damage, the interactions between MDM2 and p53 are suppressed, resulting in increased p53 activity that triggers apoptosis. Our data suggest that MDM2 might act as a general coordinator to turn off multiple negative growth regulators, including FOXO factors, when p53 senses that the DNA damage has been repaired (Fig. 7*E*). During our investigations, several studies documented a functional cross-talk between p53 and FOXO3A. In the presence of hydrogen peroxide, p53 and FOXO3A were found to form a complex (26). DNA damage was

also reported to promote FOXO3A nuclear export through the p53-dependent activation of serum and glucocorticoid-activated kinase (55). In addition, activated FOXO3A was also reported to impair the transcriptional activity of p53 but to enhance its proapoptotic function in mitochondria (56). In endothelial cells (57) and dermal fibroblasts (58), inhibition of FOXO3A by AKT or siRNA promotes senescence-like growth arrest in a p53- and p21-dependent manner. Overall, p53 and FOXO factors appear to have a complex relationship, of which the outcome is likely to depend on cellular status and environment.

Besides negative regulation of p53 activity, MDM2 is overexpressed in tumor cells and functions as an oncogene to promote cancer cell growth independently of p53 (32, 45). The present studies suggest that suppression of FOXO factors may be one of the p53-independent mechanisms by which MDM2 promotes cancer cell growth and survival (Fig. 7*E*). Decreased activity of FOXO3A and FOXO1 in prostate cancers resulting from loss of PTEN leads to a decrease in TRAIL expression, which contributes to increased survival of the prostatic tumor cells (5). Loss of p27 expression has been shown to be associated with aggressive behavior in a variety of human epithelial tumors (59, 60). Stable expression of MDM2 in H1299 cells decreased the expression of FOXO3A together with manganese superoxide dismutase and p27 (Fig. 6*A*). Knockdown of MDM2 by siRNA in H1299 cells increased the level of FOXO3A together with TRAIL (Fig. 6*B*). The studies suggest that MDM2 promotes tumorigenesis in part through down-regulation of FOXO target genes and that the targeted interruption of FOXO ubiquitination and degradation by MDM2 may represent an effective strategy for cancer prevention or therapy.

Acknowledgments—We thank the flow cytometry core facility at H. Lee Moffitt Cancer Center for FACS analyses and the microscopic core at the University of South Florida College of Medicine for imaging analyses. We also thank Lihong Chen for technical help and Dr. John Tsibris for reading the manuscript.

REFERENCES

1. Katoh, M., and Katoh, M. (2004) *Int. J. Oncol.* **25,** 1495–1500
2. Medema, R. H., Kops, G. J., Bos, J. L., and Burgering, B. M. (2000) *Nature* **404,** 782–787
3. Nakamura, N., Ramaswamy, S., Vazquez, F., Signoretti, S., Loda, M., and Sellers, W. R. (2000) *Mol. Cell. Biol.* **20,** 8969–8982
4. Schmidt, M., Fernandez de Mattos, S., van der Horst, A., Klompmaker, R., Kops, G. J., Lam, E. W., Burgering, B. M., and Medema, R. H. (2002) *Mol. Cell. Biol.* **22,** 7842–7852
5. Modur, V., Nagarajan, R., Evers, B. M., and Milbrandt, J. (2002) *J. Biol. Chem.* **277,** 47928–47937
6. Essers, M. A., Weijzen, S., de Vries-Smits, A. M., Saarloos, I., de Ruiter, N. D., Bos, J. L., and Burgering, B. M. (2004) *EMBO J.* **23,** 4802–4812
7. Kajihara, T., Jones, M., Fusi, L., Takano, M., Feroze-Zaidi, F., Pirianov, G., Mehmet, H., Ishihara, O., Higham, J. M., Lam, E. W., and Brosens, J. J. (2006) *Mol. Endocrinol.* **20,** 2444–2455
8. Sandri, M., Sandri, C., Gilbert, A., Skurk, C., Calabria, E., Picard, A., Walsh, K., Schiaffino, S., Lecker, S. H., and Goldberg, A. L. (2004) *Cell* **117,** 399–412
9. Carter, M. E., and Brunet, A. (2007) *Curr. Biol.* **17,** R113–R114
10. Barthel, A., Schmoll, D., and Unterman, T. G. (2005) *Trends Endocrinol. Metab.* **16,** 183–189
11. Kenyon, C. (2005) *Cell* **120,** 449–460
12. Dong, X. Y., Chen, C., Sun, X., Guo, P., Vessella, R. L., Wang, R. X., Chung, L. W., Zhou, W., and Dong, J. T. (2006) *Cancer Res.* **66,** 6998–7006
13. Paik, J. H., Kollipara, R., Chu, G., Ji, H., Xiao, Y., Ding, Z., Miao, L., Tothova, Z., Horner, J. W., Carrasco, D. R., Jiang, S., Gilliland, D. G., Chin, L., Wong, W. H., Castrillon, D. H., and DePinho, R. A. (2007) *Cell* **128,** 309–323
14. Tothova, Z., Kollipara, R., Huntly, B. J., Lee, B. H., Castrillon, D. H., Cullen, D. E., McDowell, E. P., Lazo-Kallanian, S., Williams, I. R., Sears, C., Armstrong, S. A., Passegue, E., DePinho, R. A., and Gilliland, D. G. (2007) *Cell* **128,** 325–339
15. Aoki, M., Jiang, H., and Vogt, P. K. (2004) *Proc. Natl. Acad. Sci. U. S. A.* **101,** 13613–13617
16. Brunet, A., Bonni, A., Zigmond, M. J., Lin, M. Z., Juo, P., Hu, L. S., Anderson, M. J., Arden, K. C., Blenis, J., and Greenberg, M. E. (1999) *Cell* **96,** 857–868
17. Brunet, A., Park, J., Tran, H., Hu, L. S., Hemmings, B. A., and Greenberg, M. E. (2001) *Mol. Cell. Biol.* **21,** 952–965
18. Rena, G., Woods, Y. L., Prescott, A. R., Peggie, M., Unterman, T. G., Williams, M. R., and Cohen, P. (2002) *EMBO J.* **21,** 2263–2271
19. Lehtinen, M. K., Yuan, Z., Boag, P. R., Yang, Y., Villen, J., Becker, E. B., DiBacco, S., de la Iglesia, N., Gygi, S., Blackwell, T. K., and Bonni, A. (2006) *Cell* **125,** 987–1001
20. Hu, M. C., Lee, D. F., Xia, W., Golfman, L. S., Ou-Yang, F., Yang, J. Y., Zou, Y., Bao, S., Hanada, N., Saso, H., Kobayashi, R., and Hung, M. C. (2004) *Cell* **117,** 225–237
21. Huang, H., Regan, K. M., Lou, Z., Chen, J., and Tindall, D. J. (2006) *Science* **314,** 294–297
22. Plas, D. R., and Thompson, C. B. (2003) *J. Biol. Chem.* **278,** 12361–12366
23. Matsuzaki, H., Daitoku, H., Hatta, M., Tanaka, K., and Fukamizu, A. (2003) *Proc. Natl. Acad. Sci. U. S. A.* **100,** 11285–11290
24. Perrot, V., and Rechler, M. M. (2005) *Mol. Endocrinol.* **19,** 2283–2298
25. Matsuzaki, H., Daitoku, H., Hatta, M., Aoyama, H., Yoshimochi, K., and Fukamizu, A. (2005) *Proc. Natl. Acad. Sci. U. S. A.* **102,** 11278–11283
26. Brunet, A., Sweeney, L. B., Sturgill, J. F., Chua, K. F., Greer, P. L., Lin, Y., Tran, H., Ross, S. E., Mostoslavsky, R., Cohen, H. Y., Hu, L. S., Cheng, H. L., Jedrychowski, M. P., Gygi, S. P., Sinclair, D. A., Alt, F. W., and Greenberg, M. E. (2004) *Science* **303,** 2011–2015
27. Yang, Y., Hou, H., Haller, E. M., Nicosia, S. V., and Bai, W. (2005) *EMBO J.* **24,** 1021–1032
28. Frescas, D., Valenti, L., and Accili, D. (2005) *J. Biol. Chem.* **280,** 20589–20595
29. Kitamura, Y. I., Kitamura, T., Kruse, J. P., Raum, J. C., Stein, R., Gu, W., and Accili, D. (2005) *Cell Metab.* **2,** 153–163
30. Haupt, Y., Maya, R., Kazaz, A., and Oren, M. (1997) *Nature* **387,** 296–299
31. Montes de Oca Luna, R., Wagner, D. S., and Lozano, G. (1995) *Nature* **378,** 203–206
32. Ganguli, G., and Wasylyk, B. (2003) *Mol. Cancer Res.* **1,** 1027–1035
33. Lin, H. K., Wang, L., Hu, Y. C., Altuwaijri, S., and Chang, C. (2002) *EMBO J.* **21,** 4037–4048
34. Pochampally, R., Fodera, B., Chen, L., Lu, W., and Chen, J. (1999) *J. Biol. Chem.* **274,** 15271–15277
35. Peng, Y., Chen, L., Li, C., Lu, W., and Chen, J. (2001) *J. Biol. Chem.* **276,** 40583–40590
36. Wang, C., Ivanov, A., Chen, L., Fredericks, W. J., Seto, E., Rauscher, F. J., III, and Chen, J. (2005) *EMBO J.* **24,** 3279–3290
37. McMasters, K. M., Montes de Oca Luna, R., Pena, J. R., and Lozano, G. (1996) *Oncogene* **13,** 1731–1736
38. Chen, J., Marechal, V., and Levine, A. J. (1993) *Mol. Cell. Biol.* **13,** 4107–4114
39. Chen, J., Lin, J., and Levine, A. J. (1995) *Mol. Med.* **1,** 142–152
40. Freedman, D. A., and Levine, A. J. (1999) *Cancer Res.* **59,** 1–7
41. Li, P., Lee, H., Guo, S., Unterman, T. G., Jenster, G., and Bai, W. (2003) *Mol. Cell. Biol.* **23,** 104–118
42. Li, P., Nicosia, S. V., and Bai, W. (2001) *J. Biol. Chem.* **276,** 20444–20450
43. Honda, R., Tanaka, H., and Yasuda, H. (1997) *FEBS Lett.* **420,** 25–27
44. Chen, L., Marechal, V., Moreau, J., Levine, A. J., and Chen, J. (1997) *J. Biol. Chem.* **272,** 22966–22973
45. Daujat, S., Neel, H., and Piette, J. (2001) *Trends Genet.* **17,** 459–464

46. Huang, H., Regan, K. M., Wang, F., Wang, D., Smith, D. I., van Deursen, J. M., and Tindall, D. J. (2005) *Proc. Natl. Acad. Sci. U. S. A.* **102,** 1649–1654
47. Yang, J. Y., Zong, C. S., Xia, W., Yamaguchi, H., Ding, Q., Xie, X., Lang, J. Y., Lai, C. C., Chang, C. J., Huang, W. C., Huang, H., Kuo, H. P., Lee, D. F., Li, L. Y., Lien, H. C., Cheng, X., Chang, K. J., Hsiao, C. D., Tsai, F. J., Tsai, C. H., Sahin, A. A., Muller, W. J., Mills, G. B., Yu, D., Hortobagyi, G. N., and Hung, M. C. (2008) *Nat. Cell Biol.* **10,** 138–148
48. Brenkman, A. B., de Keizer, P. L., van den Broek, N. J., Jochemsen, A. G., and Burgering, B. M. (2008) *PLoS ONE* **3,** e2819
49. Zhou, B. P., Liao, Y., Xia, W., Zou, Y., Spohn, B., and Hung, M. C. (2001) *Nat. Cell Biol.* **3,** 973–982
50. Feng, J., Tamaskovic, R., Yang, Z., Brazil, D. P., Merlo, A., Hess, D., and Hemmings, B. A. (2004) *J. Biol. Chem.* **279,** 35510–35517
51. Yu, Z. K., Geyer, R. K., and Maki, C. G. (2000) *Oncogene* **19,** 5892–5897
52. Li, M., Brooks, C. L., Wu-Baer, F., Chen, D., Baer, R., and Gu, W. (2003) *Science* **302,** 1972–1975
53. van der Horst, A., de Vries-Smits, A. M., Brenkman, A. B., van Triest, M. H., van den Broek, N., Colland, F., Maurice, M. M., and Burgering, B. M. (2006) *Nat. Cell Biol.* **8,** 1064–1073
54. Jin, S., and Levine, A. J. (2001) *J. Cell Sci.* **114,** 4139–4140
55. You, H., Jang, Y., You-Ten, A. I., Okada, H., Liepa, J., Wakeham, A., Zaugg, K., and Mak, T. W. (2004) *Proc. Natl. Acad. Sci. U. S. A.* **101,** 14057–14062
56. You, H., Yamamoto, K., and Mak, T. W. (2006) *Proc. Natl. Acad. Sci. U. S. A.* **103,** 9051–9056
57. Miyauchi, H., Minamino, T., Tateno, K., Kunieda, T., Toko, H., and Komuro, I. (2004) *EMBO J.* **23,** 212–220
58. Kyoung Kim, H., Kyoung Kim, Y., Song, I. H., Baek, S. H., Lee, S. R., Hye Kim, J., and Kim, J. R. (2005) *J. Gerontol. A Biol. Sci. Med. Sci.* **60,** 4–9
59. Macri, E., and Loda, M. (1998) *Cancer Metastasis Rev.* **17,** 337–344
60. Catzavelos, C., Bhattacharya, N., Ung, Y. C., Wilson, J. A., Roncari, L., Sandhu, C., Shaw, P., Yeger, H., Morava-Protzner, I., Kapusta, L., Franssen, E., Pritchard, K. I., and Slingerland, J. M. (1997) *Nat. Med.* **3,** 227–230